Robust Control for Launchers: VEGA study case

Marcos, Andrés*, Navarro-Tapia, Diego*, Simplício, Pedro* ・Bennani, Samir**

* TASC (https://www.tasc-group.com/), University of Bristol, UK
** ESA-ESTEC, Noordwijk, The Netherlands.

1. Introduction

In this article a summary of on-going activities in Europe related to atmospheric launcher thrust vector control (TVC) is given. The article focuses on the joint collaboration between the Technology for Aero-Space Control (TASC) group and the European Space Agency Technology Center (ESA-ESTEC) spanning the last 6 years –and with indispensable support from ELV, now Avio, the prime responsible for the European small launcher VEGA. The aim of the article is to provide a coherent perspective of the results related to the TVC design process, as applied to an industrial-level VEGA simulator provided by ELV/Avio that includes the VEGA baseline atmospheric TVC for one of its flown mission. Furthermore, as this joint collaboration aimed to transfer advanced robust techniques [1, 2] to industry, the article only covers the modeling, design and analysis activities more specifically oriented towards this transfer.

The layout of the paper is as follows. First, a brief state-of-practice review on launcher TVC and its problematic is performed in Section 2. This is followed by a presentation of the VEGA launcher system, mission and verification software simulation tool (Section 3). Then, the main developments are presented: robust modeling (Section 4), robust design (Section 5) and analysis (Section 6). The latter includes classical and robust verification as well as nonlinear validation via Monte Carlo campaigns.

2. Problematic and Brief Historical Overview

Launcher guidance, navigation and control (GNC) during the atmospheric phase is heavily impacted by endogenous and exogenous effects which make of this control problem a very challenging one. Among the endogenous issues the most critical ones are: flexible effects, sloshing, variations in the mass, centre of gravity and moment of inertia (MCI), non-collocation of sensors and actuators (respectively at the top and bottom of the launcher), aerodynamic instability due to vehicle's design aspects, nonlinearities in the actuators, sensors/filtering quality, and propulsion effects. And with respect to the exogenous issues: atmospheric (wind, turbulence, gust) and mission-related (e.g. dynamic pressure and heat-flux due to the high speed of the launcher during ascent). All of the previous effects are exacerbated by uncertainty on their knowledge and on the vehicle's parameters variation. For example, analysis of data recordings from the European VEGA launcher qualification flights (and similar results in the U.S. for the ARES-I) have evidenced significant modelling mismatch of the first and second mode resonances between the TVC and the filtering functions. This is especially critical for launchers as most are aerodynamically unstable vehicles due to the centre of pressure being located above the centre of mass.

Because of the above, it is hard to achieve with the current GNC industrial design approach uniform stability and performance over the entire flight in a robust manner. Furthermore, the TVC control law settings need to be updated for each flight to account for the mission-specific configuration, different payload and new trajectory. This is a very costly and time-consuming process –especially for launchers that, despite the ever more demanding missions and payloads still use TVC systems designed using a two-step classical control design state-of-practice: i.e. first design a controller for the launcher rigid-body dynamics and then in a second step, a set of bending filters to prevent excitation of its flexible modes. In addition, and compounding the design difficulty, this sequential process is done first locally (i.e. at different flight time instances throughout the ascent trajectory), and then the family of controllers are globally scheduled in an ad hoc, manual manner based on time or velocity.

This state-of-practice arises from the historical legacy of launcher development. The first launch vehicles were developed based on the German V-2 rocket during World War II. Subsequently, and driven by a frenetic technological Space Race, many of the launch vehicles families were developed: such as the Soviet R-7, Soyuz

and Proton and the US Redstone, Atlas, Titan, Delta and Saturn rockets. Indeed, the Space Race meant a significant boost to the evolution of launch vehicle technology and of the GNC architectures and algorithms required to provide reliable performance and proper TVC attitude control. During this period the main design objectives and limitations were posed [3, 4], and given the know-how at that time the aforementioned process was developed and applied using classical control (i.e. PID). For example, the US Saturn V rocket [5, 6] used in the Apollo missions, and more recently the US Ares-I flight control system [7] and the European VEGA launcher [8], all have TVC systems developed in this (local) two-step plus (global) manual-scheduling design process fashion.

Despite the above traditional approach, optimal control approaches have been used when required by the new demands of the missions/payloads, the start of a new launcher program or for technology maturation. For example, the TVC flight system of the Ariane 5 launch vehicle was initially designed using the LQG approach [9], but the limitations of this approach encouraged the application of H_∞ robust control for its atmospheric rigid-body control system [10]. This resulted in better rigid-body stability robustness, less TVC consumption and a more systematic tuning process, all of which motivated the change to H_∞ control for the evolution of the Ariane 5 launcher. This approach has been employed also by JAXA for the first-stage attitude control design of the Japanese M-V launch vehicle [11]. The main difference is that its design, while also performed in two steps, focused first on stabilizing the unstable launch vehicle plant (using a classical output feedback), and in a second step used the H_∞ approach to optimise the launcher performance.

3. VEGA: launcher, mission and tools.

The focus of this article is on launcher atmospheric phase control, which pertains the TVC of the first stage of the launcher (called P80 in VEGA, see Figure 1). Note that the main control objective is to use the thrust vector along the pitch and yaw planes to follow the offline-calculated flight trajectory (in the face of all the aforementioned challenges, uncertainties and atmospheric effects).

VEGA (Vettore Europeo di Generazione Avanzata, in English Advanced Generation European Launcher), see Figure 1, is a European small launch vehicle developed under the responsibility of ESA by ELV, now Avio (Italy). The launcher performed its maiden launch on the 13th February 2012 from the Centre Spatial Guyanais in Kourou followed by another 13 successful launches until March 2019. The 15th mission on 11th July 2019 suffered a malfunction during the ignition of the 2nd stage representing the first VEGA failed mission.

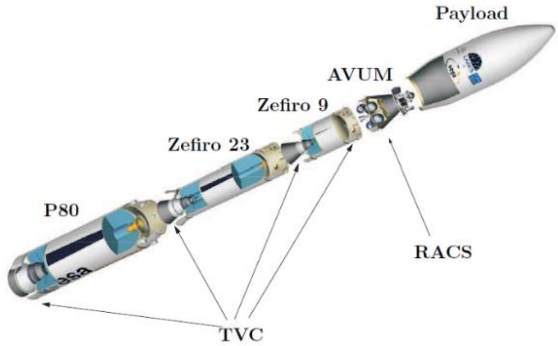

Figure 1 VEGA launcher in LARES mission configuration

3.1 VEGA launcher and mission

VEGA follows a four-stage approach formed by 3 solid propellant motors (P80, Zefiro 23 and Zefiro 9) providing thrust for the 1st, 2nd and 3rd stages, and a bi-propellant liquid engine (LPS) on the 4th stage. All four stages are controlled via TVC, located at the bottom of each stage. There is also a Roll and Attitude Control System (RACS) performing roll rate control during the propelled phases and 3-axes control during the ballistic phase.

The VEGA launcher performs a wide range of missions with specific configurations and trajectories. In the results presented in this article, the actual VEGA 5th mission (VV05) data is used [12]. The payload of this mission was the Sentinel-2A satellite, part of Europe's Copernicus Earth observation program. Reference [13] provides information on the nominal flight responses for altitude, Mach and dynamic pressure for the first atmospheric phase (P80 stage). During this first phase, VEGA reached Mach 5 and about 50 km of altitude.

3.2 VEGA nonlinear simulator

The high-fidelity, nonlinear, time-domain simulator used in the VEGA program for GNC validation purposes is characterized by [14]:

- High-fidelity 6 Degrees-of-Freedom motion
- Tail-Wag-Dog effects
- Bending and sloshing modes
- External environment (rotating Earth, winds, gusts ...)
- Disturbances (torques at separation, bias, offsets)
- Nonlinear aerodynamics (including aero-elastic effects)
- TVC system (computing delays, backlash, bias ...)
- Full code implementing actual GNC system

- Propulsion and mass-centre-inertia (MCI) properties
- Detailed inertial navigation system (INS)
- Detailed RACS models (thermal, filter quantization ...)

The nonlinear simulator used in this work (provided by ELV) is called VEGACONTROL, see Figure 2, and the two main differences with respect to the validation simulator are that it simulates only the 1st atmospheric phase of VEGA (about 110 seconds flight time for VV05) and that it is prepared for accelerated-time simulation (through protected and compiled code –the grey boxes in Figure 2). Otherwise, VEGACONTROL retains most of the validation simulator sophistication. Additionally, both allow modifying the scattering values (uncertainties and dispersions) of up to 125 launcher parameters (MCI, aerodynamics, wind profiles, INS mounting…). Each scattering variable is represented by a normalized flag (i.e. ranging between ±1 and with the zero-value indicating nominal behaviour) accessible to the user.

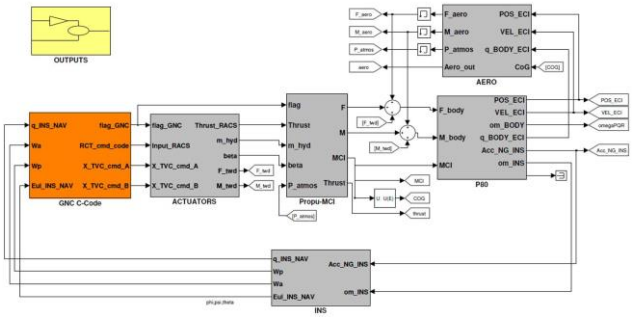

Figure 2 VEGACONTROL nonlinear simulator

4. Robust modeling for launchers

In this section, two approaches to derive robust (i.e. uncertain) models for launcher vehicles are presented. Both are based on the robust theory modeling formalism known as linear fractional transformation (LFT) [1, 2, 15]. This modeling approach allows capturing the uncertain, time-varying and/or nonlinear character of a system in a manner conducive for robust design and analysis.

The first approach [16], one of the most widely used for LFT modelling, is termed analytical since it relies on introducing standard uncertainty models in an analytical representation of the system's equations, followed by an LFT manipulation step, and concluding with a numerical substitution of the parameters' values at different points in the trajectory. This approach typically yields a large LFT dimension (i.e. number of uncertain parameters and their repetitions) but tends to produce the most accurate LFT with respect to the original system.

The 2nd approach (first used in [14] for the 3rd VEGA flight, and then detailed in [17] using the VV05) is termed grey-box as it first identifies, via time-domain simulations with VEGACONTROL, the physical parameters and uncertainty representations that best capture the system variability, and then follows the same steps as the previous approach. It yields a smaller dimension LFT and includes uncertainty correlation, but it is less accurate.

A detailed comparison of the two different LFT models for the launch vehicle shows that there are substantial differences, but that these do not invalidate the robust analyses (see section 6). Indeed, the two LFTs capture the main system features but approximate other effects at different levels of accuracy.

4.1 Analytical LFT approach (LFT-A)

Following the approach described above, reference [16] derived LFT models for the launcher $\{G_{LV}, \Delta_{LV}\}$, actuation delay $\{G_{\tau}, \Delta_{\tau}\}$, and TVC actuator $\{G_{TVC}, \Delta_{TVC}\}$ by using multiplicative uncertain representations. These $\Delta_{\#}$ models capture the percentage variation of a parameter x around its nominal value x_{NOM} by using an uncertainty flag δ_x sized by its relative range ω_x (complex or real):

$$x = x_{NOM}(1 + \omega_X \delta_X) \quad with\ \delta_X \in [-1, +1] \qquad 1$$

This is the simplest and most standard LFT approach, although using such uncertainty representation to all physical parameters yields a very high-dimensional LFT model sometimes not valid for design and/or analysis.

Figure 3 shows the graphical representation of the launcher closed loop using the full uncertainty block Δ_u (note that subsequently, when referring specifically to the launcher uncertainty block, i.e. Δ_{LV}, unless explicitly indicated by a subscript it will be considered as formed by the rigid (RB) and bending (BM) modes' uncertainty blocks shown in Δ_u). The total dimension of the LFT for the launcher $\{G_{LV}, \Delta_{LV}\}$, termed LFT-A, is 52 and accounts for 18 rigid and flexible uncertain flags. Figure 4 shows the Bode plot for the nominal and perturbed LFT-A.

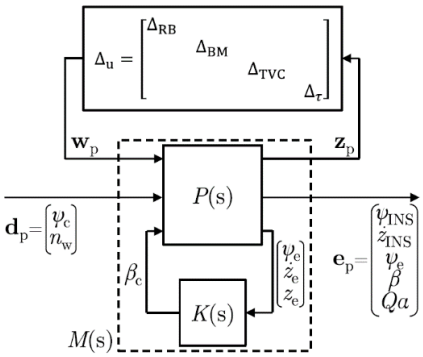

Figure 3 LFT closed-loop diagram with full Δ_u [16]

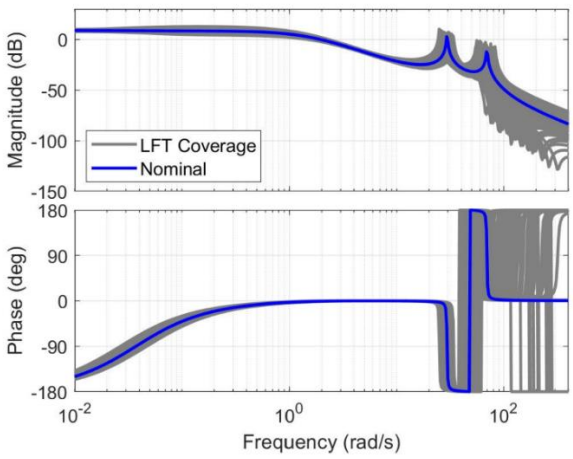

Figure 4 LFT-A (RB+BM): Bode plot

4.2 Grey-box identification LFT approach (LFT-B)

The approach was formalized in reference [17], but the reader is referred to [13] as the obtained LFT models for the launcher, delay and TVC actuator are fully detailed there (the latter two are the same as those in [16]).

The dimension of the $\{G_{LV}, \Delta_{LV}\}$ LFT using this approach, which will be termed as LFT-B to distinguish it from the previous one, is 41 and includes 11 RB+BM uncertain flags. Note that it is only 22% "smaller" than LFT-A but has 40% less number of uncertain flags (which is critical for robust design and analysis). In this approach, the uncertainty models are found by selecting a set of simulation configurations (using for example, the nominal trajectory together with minimal, nominal and maximal combinations of selected uncertain flags), running them in VEGACONTROL, and then extracting the most adequate linear or bilinear relationships between the physical parameters and the uncertain flags. An example of four of the most critical physical parameters (thrust Tc, x-coordinates for center of gravity x_{CG} and pressure x_{CP}, and dynamic pressure Q) is given in Equation 2:

$$
\begin{aligned}
T_c &= T_{c0} + \sigma_{T_c}^{\delta_{Tc}} \delta_{Tc} \\
x_{CG} &= x_{CG0} + \sigma_{X_{CG}}^{\delta_{Tc}} \delta_{Tc} \\
x_{CP} &= x_{CP0} + \sigma_{X_{CP}}^{CP_{DSP}} \delta_{x_{CP-DSP}} + \sigma_{X_{CP}}^{CP_{UNC}} \delta_{x_{CP-UNC}} \\
Q &= Q_0 + \sigma_Q^{\delta_{Tc}} \delta_{Tc} + \sigma_Q^{\delta_\rho} \delta_\rho
\end{aligned}
\qquad 2
$$

It is noted that some of the uncertain models could have been developed using knowledge of the physical system, e.g. by understanding the effect of thrust uncertainty (δ_{Tc}) and density uncertainty (δ_ρ) on dynamic pressure, but that others were not straight-forward, e.g. both x_{CG} and x_{CP} had uncertainty ($\delta x_{\#\text{-}UNC}$) and dispersion ($\delta x_{\#\text{-}DSP}$) flags but for x_{CG} it was found better to use only a dependence on δ_{Tc} as shown in Equation 2. It is highlighted that the exact uncertainty implementation in VEGACONTROL was not known but the main ones were subsequently confirmed by ELV to have been appropriately identified.

For comparison, Figure 5 shows the LFT-B Bode plot. The differences with the Bode plot for LFT-A are apparent (especially at the low-frequency region). A subsequent study identified the uncertainty approximations in LFT-B responsible for these differences. Since both LFTs were valid for analysis (and LFT-B more applicable for design due to its reduced size) no effort was made to align them closer. This shows the strengths of LFT modeling: (i) it can provide valid analysis results, see section 6, even when approximating the uncertainty effects in a rough manner, (ii) they can be easily examined, and improved if necessary, due to their modular nature (see Figure 3), and (iii) the trade-off between accuracy and efficiency (in terms of LFT size) can be very clearly understood.

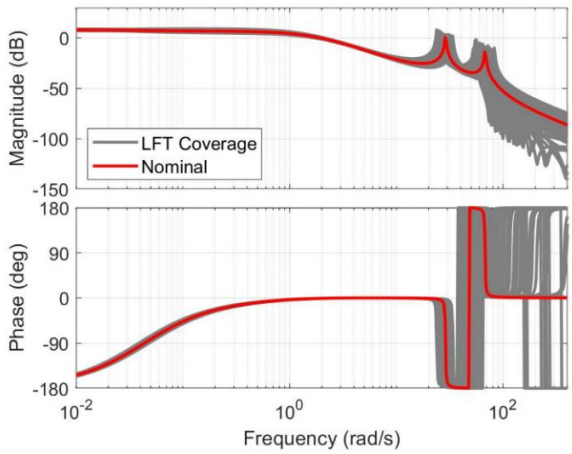

Figure 5 LFT-B (RB+BM): Bode plot [13]

5. Launcher TVC design

In this section, the TASC/ESA efforts to demonstrate the validity of the advanced robust control design techniques for VEGA are cursorily described. Sub-section 5.1 presents ELV's industrial VEGA baseline controller, followed by sub-section 5.2 describing a process termed as legacy-recovery. This process uses a new robust control design framework and the same RB VEGA architecture together with information derived from understanding of the closed-loop VEGA transfer functions. Sub-section 5.3 then shows (from a standard, sequential two-step design process) how the new framework can be used to augment the capabilities of the VEGA controller, resulting in better performance versus robustness trade-off.

5.1 Classical design: ELV baseline Rigid & Flexible (K_{ELV})

The VEGA control system is composed of the TVC and RACS subsystems. The former uses measurements from the INS unit and computes the nozzle actuator deflections required to follow the attitude commands provided by the guidance function. For VEGA, as for most launchers, there are two identical TVC actuators each affecting either the pitch or yaw planes. The RACS subsystem in VEGA is formed by a set of six thrusters, and its operating aims were described in sub-section 3.1. During the atmospheric phase, the guidance is performed in an open-loop configuration following a pre-programmed trajectory, but this strategy leads to deviations from the nominal trajectory, which must be corrected in upper phases of the flight. In this article only the TVC component and atmospheric phase is covered. And, as shown in [8], ELV follows the standard, two-step design approach for VEGA: first, designing a controller for the rigid-body (RB) motion and then bending filters to attenuate the flexible effects.

The high-level objectives of the flight control system (and, indirectly, of the TVC) are to: (i) manage, guide, and control the launcher to achieve orbital conditions, (ii) keep load levels limited in the face of disturbances, (iii) optimize the trade-off between consumption, tracking, and loads, and (iv) perform the mission in a safe way in nominal and dispersed flight. See references [13, 16] for the detailed TVC control design objectives and rationale during the atmospheric ascent phase.

The baseline controller used in this work, developed by ELV [8], uses for each channel (pitch and yaw) the exact same controller. As shown in Figure 6, it is formed by four RB proportional and derivative gains in charge of providing stability and performance in attitude and drift, plus four numerically optimized filters that: improve the low-frequency RB stability margins, $H_1(s)$; add derivative action to compute the attitude rate error signal ($\dot{\psi}_e$), $H_2(s)$; notch the first bending mode, $H_3(s)$; and attenuate the upper bending modes (BM), $H_4(s)$. The channels are assumed uncoupled except in presence of roll rate, when a compensation term is added to limit its maximum range.

As shown in Figure 6, the TVC uses as inputs the tracking errors for the attitude (ψ_e), drift (z) and drift rate ($\dot{z}$), and as output the nozzle deflection ($\beta_{\psi c}$). The filters $H_\#(s)$ have a dynamical order of 4, 4, 14 and 2 respectively, resulting in a total of 26 states (since $H_4(s)$ is repeated twice). Some are easily derived but others are more complicated. As aforementioned, the RB component is formed by four control gains $\{K_{\Psi_P}, K_{\Psi_D}, K_z, K_{\dot{z}}\}$.

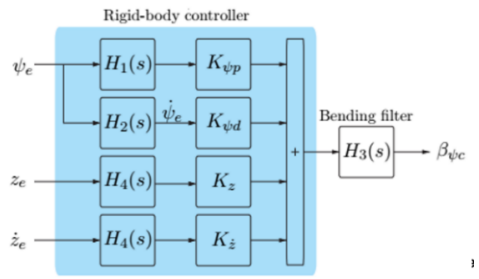

Figure 6 VEGA baseline ELV TVC [8]

Controllers are designed at 9 different flight times, i.e. at time t=5s and every 10 seconds in the [20-90]s flight region. Then, the controllers are discretized, and all gains and filters' coefficients scheduled throughout the flight to cope with the system time-varying dynamics [8]. The scheduling parameter is NGV, the non-gravitational velocity (but it can also be directly time from launch). All the tunings used here are from VEGA VV05 mission [12].

5.2 Structured-H_∞ design: Rigid-Body legacy recovery

In this section, the design of the VEGA TVC is recast as a robust control problem [1, 2] using the structured H_∞ approach [18, 19]. This synthesis technique allows to specify the dimension, or even a precise architecture, of the controller while due to its H_∞ optimization foundation retaining advantageous methodological and trade-off (between performance and robustness) capabilities. In addition, it includes additional capabilities that will be used later in sub-section 5.3 to augment the control design. Significant results using this approach have appeared in the last decade, including relevant Space-flown missions [20, 21] piloted flight tests (TASC/JAXA) [22], and launcher control design for non-industrial simulators [23, 24].

The aim of the recasting is to recover the four RB gains from the baseline design using the same control architecture (Figure 6). That is, perform a legacy recovery design using the robust control formulation. This is done in order to increase confidence by industry and thus facilitate the transfer of the approach. Note that this is not a simple reverse engineering of the VEGA controller, rather, the recovery design is based on both, an analytical understanding of the launcher problem (via transfer function analysis) and a systematic weight tuning of the objectives using the robust formulation.

The VEGA legacy recovery was first presented in [18], however, the evolved interconnection (IC) of [13], see Figure 7, is preferred since it allows for improved understanding. The interconnection is quite general (i.e.

applicable to most launchers' TVC design) and uses standard weights to define the input/output objectives. The importance of the recovery study is that it allowed defining this general interconnection, and then showing that the structured H_∞ approach (based on a non-smooth optimization algorithm) could be used to recover exactly the baseline gains without using exact information to initialize the optimization but just guided by the specified objectives as defined by the used through the weights.

The results in [13] showed that the recovery was almost identical, i.e. within 1% of the original gains.

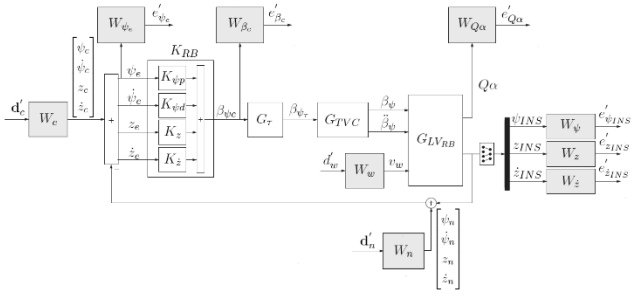

Figure 7 Structured-H_∞ design: legacy recovery IC

5.3 Structured-H_∞ design: robust sequential design (K_{ROB})

Now, the developed legacy IC shown above is gradually augmented with additional blocks (in blue background) that improve the information on the system. Then, the weights are retuned to improve the design (by enhancing its robustness while maintaining, or even improving, its performance). The augmentation was performed in two steps emulating the standard, industrial design process.

<u>**Step-1**: robust rigid-body design</u> ($K_{rob\text{-}step1}$)

First, see [25], the legacy IC is augmented by a model capturing the statistical wind expectation, G_w from [15], and the LFT models $\{\Delta_\tau, \Delta_{TVC}, \Delta_{LV}\}$ from sub-section 4.2. The augmented IC_{RB} is shown in Figure 8 with the new blocks in cyan. The weights are tuned at the same 9 flight times as the baseline, and then discretized and scheduled in the same manner. The results, see sub-section 6.1, indicate quite an improvement with respect to the gains used for K_{ELV} in both terms, performance and robustness.

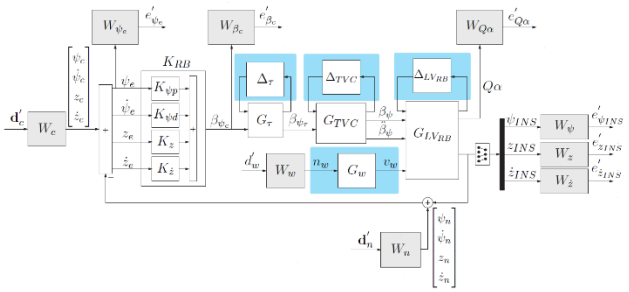

Figure 8 Structured-H_∞ design: augmented step-1 IC_{RB}

<u>**Step-2**: robust flexible filter design</u> ($K_{rob\text{-}step2}$)

For the 2nd step, the new RB gains are hold fixed and a new bending filter $H_3(s)$ is introduced to be tuned by the structured H_∞ optimizer. This new block is highlighted in cyan in the new IC_{BM} interconnection, see Figure 9. Notice that in this case the launcher block G_{LV} includes the flexible dynamics (as opposed to the previous ICs).

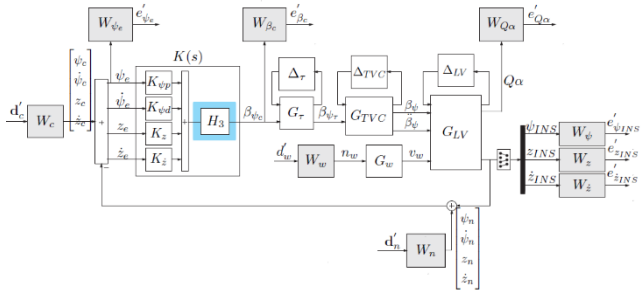

Figure 9 Structured-H_∞ design: augmented step-2 IC_{BM}

The definition of the BM filter is given in Equation 3, and is based on the knowledge that in VEGA this filter performs phase stabilization for the 1st BM and gain stabilization of upper modes –with added complexity due to proximity of the former to the rigid-body bandwidth. For this reason, two tunable Notch-filters (with tunable parameters $\zeta_{\#i}$ and $\omega_{\#i}$ for i=1,2) are used plus a fixed 6th order low-pass filter derived using VV05 BM data:

$$H_3(s) = \prod_{i=1}^{2} \frac{s^2 + 2\zeta_{ni}\omega_{ni}s + \omega_{ni}^2}{s^2 + 2\zeta_{di}\omega_{di}s + \omega_{di}^2} \left(\frac{0.335s^2 + 26.4s + 55^2}{s^2 + 44s + 55^2} \right)^3 \qquad 3$$

6. Robust analysis for launcher

In this section a summary is presented of the verification and validation (V&V) results for the previous designs. Typically, verification relies on classical linear analyses, followed by validation which is based on the standard Monte-Carlo (MC) approach (using a nonlinear, high-fidelity, time-domain simulator of the system). In those cases where knowledge and processes are available, then an in-between analysis step is performed based on the use of advanced linear robust analyses.

The above V&V process was followed in the three TASC/ESA projects that span the results in this article, but the presentation order in here is changed in order to highlight the capability of robust analysis techniques to provide further understanding. Indeed, these robust techniques complement, and help bridge, the nonlinear Monte-Carlo (sub-section 6.1) and the classical linear analyses (sub-section 6.2) by providing detailed robust stability and performance insights (sub-section 6.3).

6.1 Classical nonlinear: Monte-Carlo campaign

This analysis step is the last one performed in any V&V process, and it is the one industry relies the most. Well known limitations of MC campaigns are that they are inadequate for worst-case identification and that they do not provide information to improve the design beyond statistical binomial (yes/no) guarantees.

With respect to the designs from Section 5, Figure 10 and Figure 11 show the launcher structural load resilience (Qα boundary) for the baseline K_{ELV} (5.1) and the sequential 1st step $K_{rob\text{-}step1}$ (5.3) controllers. Since these two designs are equal except for the four RB gains, this is the best way to compare the improvements.

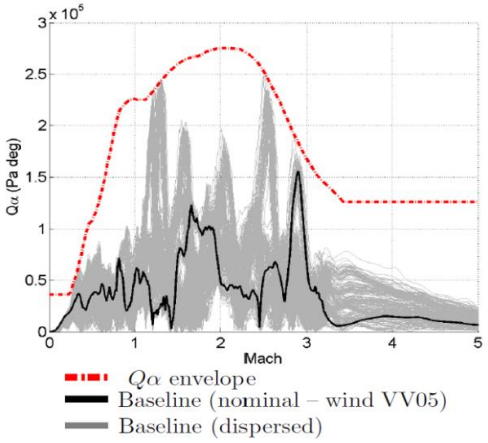

Figure 10 MC analysis: Qα response, K_{ELV} [11]

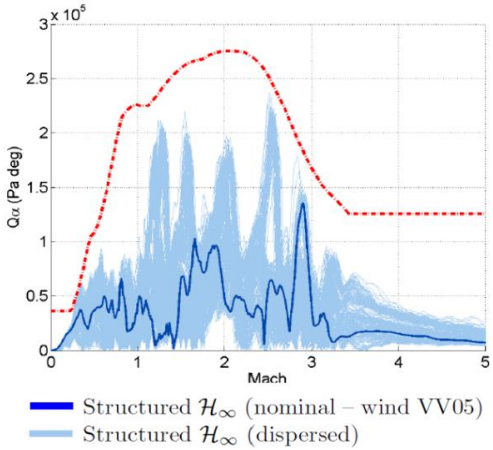

Figure 11 MC analysis: Qα response, $K_{rob\text{-}step1}$ [13]

Both controllers undergo the same four MC campaigns (all with the same 500 random uncertainty scatterings but a different wind profile [13]). As seen in the figures the new RB gains allow to improve the nominal response (performance) as well as the controller robustness. The latter can be quantitative measured by looking at the distance from the peaks to the Qα boundary –which is safely further away for the new RB controller $K_{rob\text{-}step1}$.

6.2 Classical linear: gain/phase margins and Nichols

The following linear analyses, typically carried out during the design phase, are the most widespread, easy to perform and are indeed the standard in industrial V&V. Well-known gain/phase margins analyses are used (see references [13, 16, 25]) but in launcher control it is more standard to use Nichols plots, Figure 12 and Figure 13. These figures use respectively LFT-A+ and LFT-B+ allowing to also compare their effect on the results (the '+' indicates the LFTs include the Δ_τ and Δ_{TVC} blocks shown in Figure 3). Figure 12 is across the 9 time-instances used for the VEGA TVC design, while Figure 13 is at time t=60s (near maximum Qα) but across uncertainty scattering.

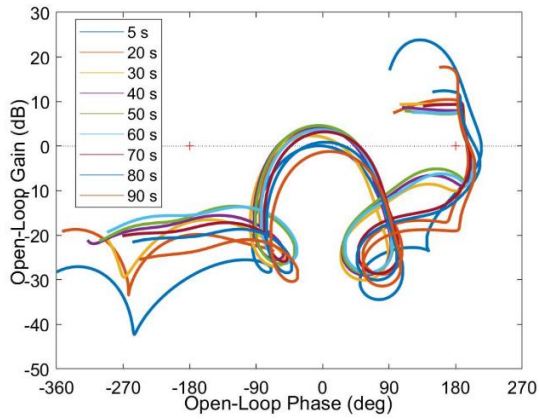

Figure 12 Classical analysis: Nichols, {K_{ELV}, LFT_{A+}}

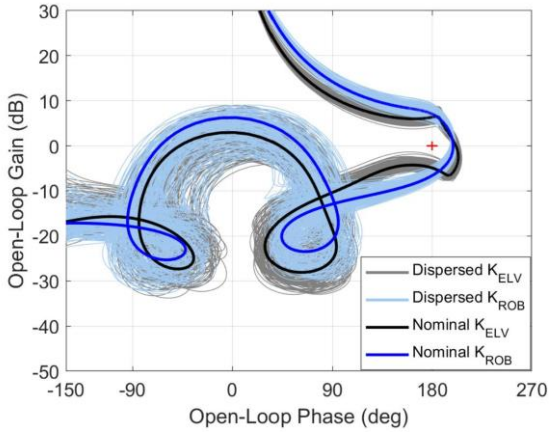

Figure 13 Classical analysis: $Nichols_{60s}$ {K_{ELV}/K_{ROB}, LFT_{B+}}

By comparing between the color lines in Figure 12 and the grey/black ones in Figure 13, a qualitative assessment is made of K_{ELV} robustness to time variation (Figure 12) and to uncertainty variation (Figure 13). On the other hand, comparing the grey/black to the light-blue/blue lines, then the assessment is between K_{ELV} and K_{ROB}. In this case, the Nichols plots of Figure 13 show that the main improvement of K_{ROB} is a larger gain attenuation for

the high-frequency gain margin (HF-GM, i.e. the distance to the critical point at 180° from below is augmented). Also, although not shown in here for space limitations, a subsequent joint rigid-bending design approach also resulted in better 1st bending mode phase (BM1).

6.3 Advanced linear: robust stability and performance

It must be highlighted that the analyses shown in 6.1 and 6.2 do not yield much insight on how to improve the designs (if re-design is necessary). And unless the designer does thorough loop-at-a-time analyses (i.e. including many parameter combinations and coupling loops), it will not be easy to understand where to improve them –e.g. which uncertainty or controller component is more critical. This is precisely one of the things that robust analysis tools can help address. For example, Figure 14 shows on the top plot the μ-analysis robust stability (RS) bounds for {K_{ELV}, LFT-A+} at time t=60 sec. Since the μ upper bound is above 1, this indicates that the closed-loop system is not guaranteed to be RS for the full uncertainty range (Figure 10 showed peaks very close to the boundary, but other MC campaigns yielded violations). Looking at the frequency axis it is seen that the issue is with the phase margin (PM) and BM1. Further, the bottom plot shows an RS sensitivity analysis specifically showing the contribution from 13 of the uncertain parameters used in LFT-A+. It is direct now to identify the more critical parameters, and at which frequencies, thus facilitating the designer's task.

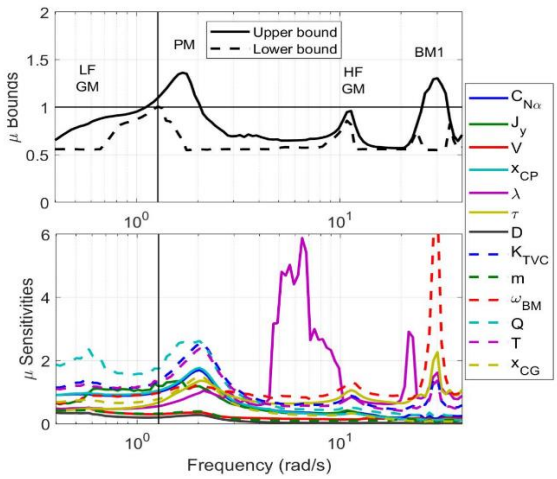

Figure 14 Advanced analysis: RS_{60s} {K_{ELV}, LFT_{A+}} [16]

Similar to the top plot in Figure 14, Figure 15 shows the RS across the 9 design times but using LFT-B+. Notice the similarities (i.e. same frequency critical areas and similar HF-GM and BM1 peaks), but also the differences (the PM peak around 10^0 rad/s is now below 1). This is an indication that care must always be used when deriving LFT models and using them for robust analysis –since the quality of the latter (and hence its reliability) is determined by the accuracy of the former. In the present case, the difference is acceptable as the PM values are also cross-checked via Nichols (see sub-section 6.2) and the LFT approximations clearly understood. This is the reason why robust analysis methods must be seen as complementary and not substitutive of traditional ones.

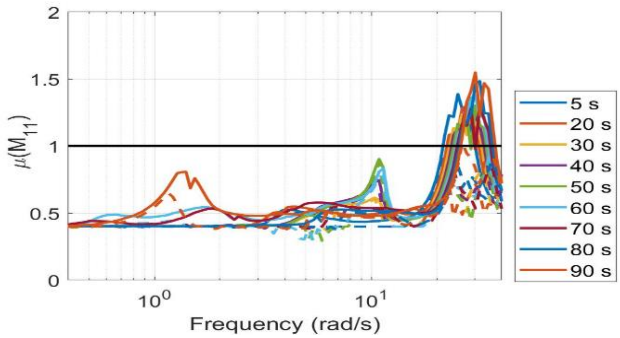

Figure 15 Advanced analysis: RS_{time} {K_{ELV}, LFT_{B+}}

Finally, Figure 16 shows the RS analysis with LFT-B+ at t=60 sec for the K_{ELV} and K_{ROB} controllers, but critically using newer RS algorithms (i.e. the previous plots used those implemented in *robuststab* from the 2015 Robust Control Toolbox [26], while the new one those in *robstab* from the 2016 release [27]). The results, equivalent to those in Figure 13 but with robustness analytical guarantees, confirm that K_{ROB} improves the HF-GM and provides the same BM1 degradation. More interestingly, compared to Figure 15 (or Figure 14), the RS analysis is now less conservative for BM1 (i.e. the difference between the upper UB and lower LB bounds is closer and below 1). This is the result of the new RS algorithms and shows that for this analysis configuration K_{ELV} is also robustly stable (as opposed to Figure 14). More advanced analyses based on IQC [28] (not shown here) demonstrated that the issue for K_{ELV} is its RS when time-variation is considered.

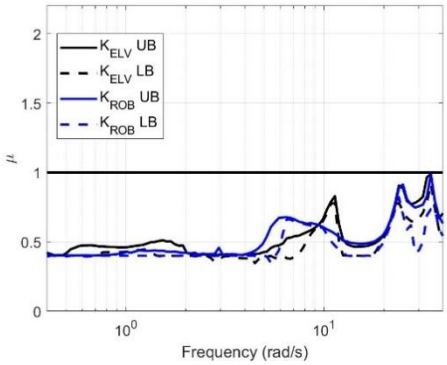

Figure 16 Advanced analysis: RS_{60s} {K_{ELV}/K_{ROB}, LFT_B}

7. Conclusion

An overview has been given on recent TASC/ESA activities aimed at consolidating robust modeling, design and analysis techniques for launchers. As one of the main objectives was to transfer the techniques to industry (specifically to ELV/Avio), the VEGA launcher was selected as the application case, and the results were verified in a high-fidelity, nonlinear simulator provided by ELV (and comparable in sophistication to the one used for validation of its controllers). The results provide a comprehensive presentation of the importance of these techniques in providing improved insight and additional design capabilities for launcher atmospheric TVC design.

8. Acknowledgement

The authors gladly acknowledge and thank the support by C. Roux at ELV/Avio, the prime of VEGA, and ESA's funding through contracts No. 4000111052/14/NL/GLC/al, 4000114460/15/NL/MH/ats and 4000119571/17/NL/MH.

参 考 文 献

1) Zhou, K., Doyle, J.C., and Glover, K. Robust and Optimal Control. Prenticel-Hall, Englewood Cliffs, NJ, 1996.
2) S. Skogestad and I. Postlethwaite, Multivariable Feedback Control: Analysis and Design. John Wiley & Sons, 2005
3) R. F. Hoelker, "Theory of Artificial Stabilization of Missiles and Space Vehicles with Exposition of Four Control Principles," NASA TN D-555, June 1961
4) A. L. Greensite, "Analysis and Design of Space Vehicle Flight Control Systems. Volume VII - Attitude Control During Launch," NASA Contractor Report CR-826, 1967
5) J. A. Frosch and D. P. Vallely, "Saturn AS-501/S-IC flight control system design," Journal of Spacecraft and Rockets, vol. 4, no. 8, pp. 1003–1009, August 1967
6) W. Haeussermann, "Description and performance of the Saturn launch vehicle's navigation, guidance and control system," NASA TN D-5869, July 1970
7) J. Jang, A. Alaniz, R. Hall, N. Bedrossian, C. Hall, S. Ryan, and M. Jackson, "Ares I flight control system design," AIAA GNC Conference, August 2010
8) C. Roux and I. Cruciani, "Scheduling schemes and control law robustness in atmospheric flight of VEGA launcher," 7th ESA International Conference on Spacecraft Guidance, Navigation and Control Systems, June 2008
9) H. Klotz, "Ariane 5 dynamics and control," 12th IFAC Symposium on Automatic Control in Aerospace, September 1992, pp. 227–233s
10) S. Mauffrey, P. Meunier, F. Seillier, M. Ganet-Schoeller, and I. Rongier, "H_∞ control for Ariane 5 Plus launcher: the industrialisation of a new technology," 5th International Conference on Launcher Technology, November 2003
11) Y. Morita and J. Kawaguchi, "Attitude control design of the M-V rocket," Philosophical Transactions: Mathematical, Physical and Engineering Sciences, vol. 359, no. 1788, pp. 2287–2303, 2001
12) Arianespace, "VEGA Flight VV05," 2015, http://www.arianespace.com/mission/vega-flight-vv05/.
13) D. Navarro-Tapia, A. Marcos, P. Simplício, S. Bennani, C.Roux, "Legacy recovery and robust augmentation structured design for the VEGA launcher," International Journal of Robust and Nonlinear Control, Vol. 29, Iss.11, pp. 3363-3388, July 2019
14) A. Marcos, P. Rosa, C. Roux, M. Bartolini, and S. Bennani, "An overview of the RFCS project V&V framework: Optimization-based and linear tools for worst-case search," CEAS Space Journal, vol. 7, no. 2, pp. 303–318, 2015
15) Doyle, J., Packard, A., Zhou, K., "Review of LFTs, LMIs and μ," 30th IEEE Conference on Decision and Control, Brighton (UK), December 1991
16) P. Simplício, S. Bennani, A. Marcos, C. Roux, X. Lefort, "Structured Singular-Value Analysis of the VEGA Launcher in Atmospheric Flight," AIAA Journal of Guidance, Control and Dynamics, vol. 39, no. 6, pp. 1342-1355, June 2016
17) A. Marcos, S. Bennani, C. Roux, "LPV modeling and LFT Uncertainty Identification for Robust Analysis: application to the VEGA Launcher during Atmospheric Phase," 1st IFAC Workshop on Linear Parameter Varying Systems, Grenoble, France, October 2015
18) D. Navarro-Tapia, A. Marcos, S. Bennani, C. Roux. "Structured H_∞ control design for the VEGA launch vehicle: recovery of the legacy control behavior," 10th ESA GNC Conference, 2017, Salzburg, Austria
19) P. Apkarian and D. Noll, "Nonsmooth H_∞ synthesis," IEEE Transactions Automatic Control. 2006;51(1):71-86
20) A. Falcoz, C. Pittet, S. Bennani, A. Guignard, C. Bayart, B. Frapard, "Systematic design methods of robust and structured controllers for satellites," CEAS Space Journal, 2015;7(3):319-334
21) C. Pittet and P. Prieur, "Structured accelero-stellar estimator for microscope drag-free mission," Advances in Aerospace Guidance, Navigation and Control: Selected Papers of the Third CEAS Specialist Conference on GNC held in Toulouse. Cham, Switzerland: Springer International Publishing; 2015:591-604
22) A. Marcos and M. Sato, "Flight testing of a structured H_∞ controller: an EU-Japan collaborative experience," 1st IEEE Conference on Control Technology and Applications (CCTA); 2017; Mauna Lani, (HI, USA)
23) M. Knoblauch, D. Saussié, C. Bérard, "Structured H_∞ control for a launch vehicle," American Control Conference; 2012; Montréal, Canada
24) D. Saussié, Q. Barbès, C. Bérard, "Self-scheduled and structured H_∞ synthesis: a launch vehicle application," American Control Conference; 2013; Washington, DC.
25) D. Navarro-Tapia, "Robust and Adaptive TVC Control Design Approaches for the VEGA Launcher", PhD Thesis, Department Aerospace Engineering, University of Bristol, UK, June 2019
26) G. Balas, R. Chiang, A. Packard, M. Safonov "Robust Control Toolbox: user's guide," The MathWorks, Inc. 2015
27) "Robust Control Toolbox Release Notes R2016b," The MathWorks, Inc, 2016
28) J. Veenman, C.W. Scherer, H. Köroğlu, "Robust stability and performance analysis based on integral quadratic constraints," European Journal of Control 31 (2916):1-32